

The Peroxisome Proliferator-Activated Receptor γ /Retinoid X Receptor α Heterodimer Targets the Histone Modification Enzyme PR-Set7/Setd8 Gene and Regulates Adipogenesis through a Positive Feedback Loop^{∇†}

Ken-ichi Wakabayashi,^{1,4} Masashi Okamura,² Shuichi Tsutsumi,¹ Naoko S. Nishikawa,³ Toshiya Tanaka,² Iori Sakakibara,² Jun-ichi Kitakami,³ Sigeo Ihara,³ Yuichi Hashimoto,⁴ Takao Hamakubo,⁵ Tatsuhiko Kodama,⁶ Hiroyuki Aburatani,¹ and Juro Sakai^{2*}

Genome Science Division,¹ Metabolism and Endocrinology Division,² Dynamical Bioinformatics Division,³ Membrane Protein Division,⁵ and Vascular System Division,⁶ Laboratory of Systems Biology and Medicine, Research Center for Advanced Science and Technology, University of Tokyo, 4-6-1, Komaba, Meguro-ku, Tokyo 153-8904, Japan, and Institute of Molecular & Cellular Biosciences, University of Tokyo, 1-1-1 Yayoi, Bunkyo-ku, Tokyo 113-0032, Japan⁴

Received 5 December 2008/Returned for modification 17 January 2009/Accepted 18 April 2009

Control of cell differentiation occurs through transcriptional mechanisms and through epigenetic modification. Using a chromatin immunoprecipitation-on-chip approach, we performed a genome-wide search for target genes of peroxisome proliferator-activated receptor γ (PPAR γ) and its partner protein retinoid X receptor α during adipogenesis. We show that these two receptors target several genes that encode histone lysine methyltransferase SET domain proteins. The histone H4 Lys 20 (H4K20) monomethyltransferase PR-Set7/Setd8 gene is upregulated by PPAR γ during adipogenesis, and the knockdown of PR-Set7/Setd8 suppressed adipogenesis. Intriguingly, monomethylated H4K20 (H4K20me1) levels are robustly increased toward the end of differentiation. PR-Set7/Setd8 positively regulates the expression of PPAR γ and its targets through H4K20 monomethylation. Furthermore, the activation of PPAR γ transcriptional activity leads to the induction of H4K20me1 modification of PPAR γ and its targets and thereby promotes adipogenesis. We also show that PPAR γ targets PPAR γ 2 and promotes its gene expression through H4K20 monomethylation during adipogenesis through a feedback loop.

Adipocytes play a central role in energy balance, both as reservoirs of fuel and as endocrine cells, secreting factors that regulate whole-body energy metabolism. Because of the rising incidence of obesity, understanding the adipocyte is increasingly important. The process of adipocyte differentiation represents the extraordinarily coordinated regulation of multiple transcriptional systems that direct multipotent stem-cell precursors to differentiate into fully mature, functionally distinct cell types.

The 3T3-L1 preadipocyte cell line has been one of the most well-characterized and widely used models for studying adipocyte differentiation (7). C/EBP β and C/EBP δ are induced very early during differentiation, and these in turn activate two critical proadipogenic transcription factors, peroxisome proliferator-activated receptor γ (PPAR γ) and C/EBP α . PPAR γ and C/EBP α mutually stimulate each other and mediate the transition to the adipocyte phenotype (6, 15, 32). Recently, a number of transcription factors have been identified as regulators of adipogenesis, including GATA2 (30, 31), the Krüppel-like factor (KLF) family (2, 20, 24), and Nr2f2 (35).

PPAR γ , a prototypical member of the nuclear receptor su-

perfamily, is activated by natural ligands, such as arachidonic acid metabolites and fatty acid-derived components, and by the insulin-sensitizing thiazolidinedione drugs. In white and brown preadipocyte cell lines, the activation of PPAR γ by thiazolidinediones results in robust differentiation into adipocytes. The action of PPAR γ is mediated by two protein isoforms: the widely expressed PPAR γ 1 and PPAR γ 2, which is restricted to adipose tissue. The expression of each isoform is driven by a specific promoter that confers the distinct tissue-specific expression and regulation. These isoforms are transcribed from a single gene and differ only by an additional 28 amino acids (30 in mice) in the N terminus of PPAR γ 1 (5, 13, 36). Despite these structural differences, no clear functional differences between these two isoforms in adipogenesis have been identified (21).

Epigenetic determinants control the accessibility of promoter chromatin and establish lineage-specific heritable states of gene expression through the modulation of DNA methylation and posttranslational modification of core histones (9, 17). Therefore, the expression and activities of histone-modifying enzymes should be distinctly regulated during adipocyte differentiation. The methylation of lysine residues in histones is an important epigenetic event that correlates with functionally distinct regions of chromatin. Setdb1 and Setd8 are the histone lysine methyltransferases (HKMTs) that trimethylate histone H3K9 and monomethylate histone H4K20, respectively. Trimethylated H3K9 is considered a hallmark of a condensed chromatin state and transcriptionally silences euchromatin (17). Monomethylated H4K20 (H4K20me1) has been impli-

* Corresponding author. Mailing address: Metabolism and Endocrinology Division, Laboratory of Systems Biology and Medicine, Research Center for Advanced Science and Technology, University of Tokyo, 4-6-1, Komaba, Meguro-ku, Tokyo 153-8904, Japan. Phone: 81-3-5452-5472. Fax: 81-3-5452-5429. E-mail: jmsakai-tyk@umin.ac.jp.

† Supplemental material for this article may be found at <http://mc.manuscriptcentral.com/mcb>.

∇ Published ahead of print on 4 May 2009.

cated in transcriptional activation and gene silencing. Recent studies showed a strong correlation between H4K20me1 and gene activation in the regions downstream of the transcription start site, consistent with it being an activation marker (1). It is tempting to speculate that epigenetic mechanisms also potentiate distinct functional states of PPAR γ target genes and that PPAR γ regulates the expression of genes encoding histone modification enzymes. An epigenetic mechanism could, for example, act downstream of PPAR γ and constitute a post-selection mechanism for potential PPAR γ -responsive genes by allowing or preventing histone modification.

To gain more insight into PPAR γ -dependent transcriptional programs in adipogenesis, we undertook the genome-wide identification of direct target genes of PPAR γ and its retinoid X receptor α (RXR α) partner. We used a combination of chromatin immunoprecipitation-on-chip (ChIP-chip) analysis and gene expression profiling with oligonucleotide microarrays during adipogenesis in 3T3-L1 cells. Our results identify *Ppar γ 2* as a direct target of PPAR γ which activates the transcription of PPAR γ 2. PPAR γ also binds to the promoters of a number of genes that encode SET domain protein lysine methyltransferases and regulates their transcription. This suggests a profound role for PPAR γ in the epigenetic control of adipogenesis.

MATERIALS AND METHODS

Antibodies. Mouse monoclonal immunoglobulin G (IgG)-A3409 against human PPAR γ and IgG-K8508 against human RXR α were raised in our laboratory by immunizing separate mice with peptides representing residues 3 to 108 of human PPAR γ 1 and 2 to 133 of human RXR α , respectively. The specificities of these were confirmed: IgG-A3409 does not cross-react with PPAR α or PPAR δ , and IgG-K8508 does not cross-react with RXR β or RXR γ (see Fig. S1 in the supplemental material). A list of the other antibodies used in this article is shown in the supplemental material experimental procedures.

Cell culture and staining. 3T3-L1 preadipocytes and NIH 3T3 cells were purchased from ATCC and maintained in Dulbecco's modified Eagle's medium supplemented with 10% fetal bovine serum (basal medium). 3T3-L1 cell differentiation into adipocytes was induced by the treatment of confluent cells first for 2 days with insulin (1 μ g/ml), 0.25 μ M dexamethasone (DEX), and 0.5 mM isobutylmethylxanthine (MDI cocktail) in basal medium. For 3T3-L1 cells were cultured for 2 days with insulin (1 μ g/ml) alone in the same medium. The cells were then returned to the basal medium, which was replenished every other day. Adipogenesis in transfected NIH 3T3 cells was induced by treatment for 2 days with MDI or 5 μ M troglitazone in basal medium. The cells were then returned to the basal medium, which was replenished every other day. The cells were stained with Oil Red O (ORO) as described in the supplemental material experimental procedures.

ChIP. For ChIP using anti-PPAR γ , RXR α , C/EBP α , or C/EBP β antibody, 3T3-L1 cells at the indicated times of differentiation were cross-linked with 1% formaldehyde for 10 min at room temperature and were prepared for ChIP as described previously (11). For ChIP using anti-Ach3, Ach4, H3K4me3, or H4K20me1 antibody, the nuclei of 3T3-L1 cells were prepared by centrifugation through a sucrose gradient and were digested with MNase (TaKaRa). After centrifugation, the supernatant was used for ChIP.

ChIP-chip, ChIP-seq, and ChIP-qPCR analysis. For ChIP-chip, ChIP samples were amplified by in vitro transcription, labeled with biotin and hybridized to oligonucleotide tiling arrays (Affymetrix) as described previously (8, 12). ChIP-sequencing analysis (ChIP-seq) sample preparation for sequencing was performed according to the manufacturer's instructions (Illumina). ChIP samples were also analyzed by gene-specific quantitative real-time PCR (qPCR) analyses. The results were normalized to cyclophilin levels in control DNA, and the ChIP was performed with specific antibody (*n*-fold enrichment) as described previously (11, 25) or presented as input percent. The method for qPCR has been described previously (11). All primer sequences used in this article are available in Table S4 in the supplemental material. The details are described in the supplemental material experimental procedures.

Computational data analysis. The details of the methods for MAT analysis, MEME analysis, gene set enrichment analysis (GSEA), and signal ratio of ChIP-seq are described in the supplemental material experimental procedures.

Transcriptome microarray analysis of 3T3-L1 cells. For genome-wide transcription analysis, a GeneChip Mouse Genome 430 2.0 array (Affimetrix) was used as described previously (23).

Method of network-based clustering of expressed genes with gene ontology. The details of the method of the clustering analysis are described in the supplemental material experimental procedures.

RNA interference. To deplete cellular PPAR γ , Setdb1, or Setd8, duplexes of Stealth Select small interfering RNAs (siRNAs) targeting each protein were purchased from Invitrogen. HiPerfect reagent (Qiagen) was used for the transfection according to the manufacturer's instructions with modifications. Details and siRNA information are available in the supplemental material experimental procedures.

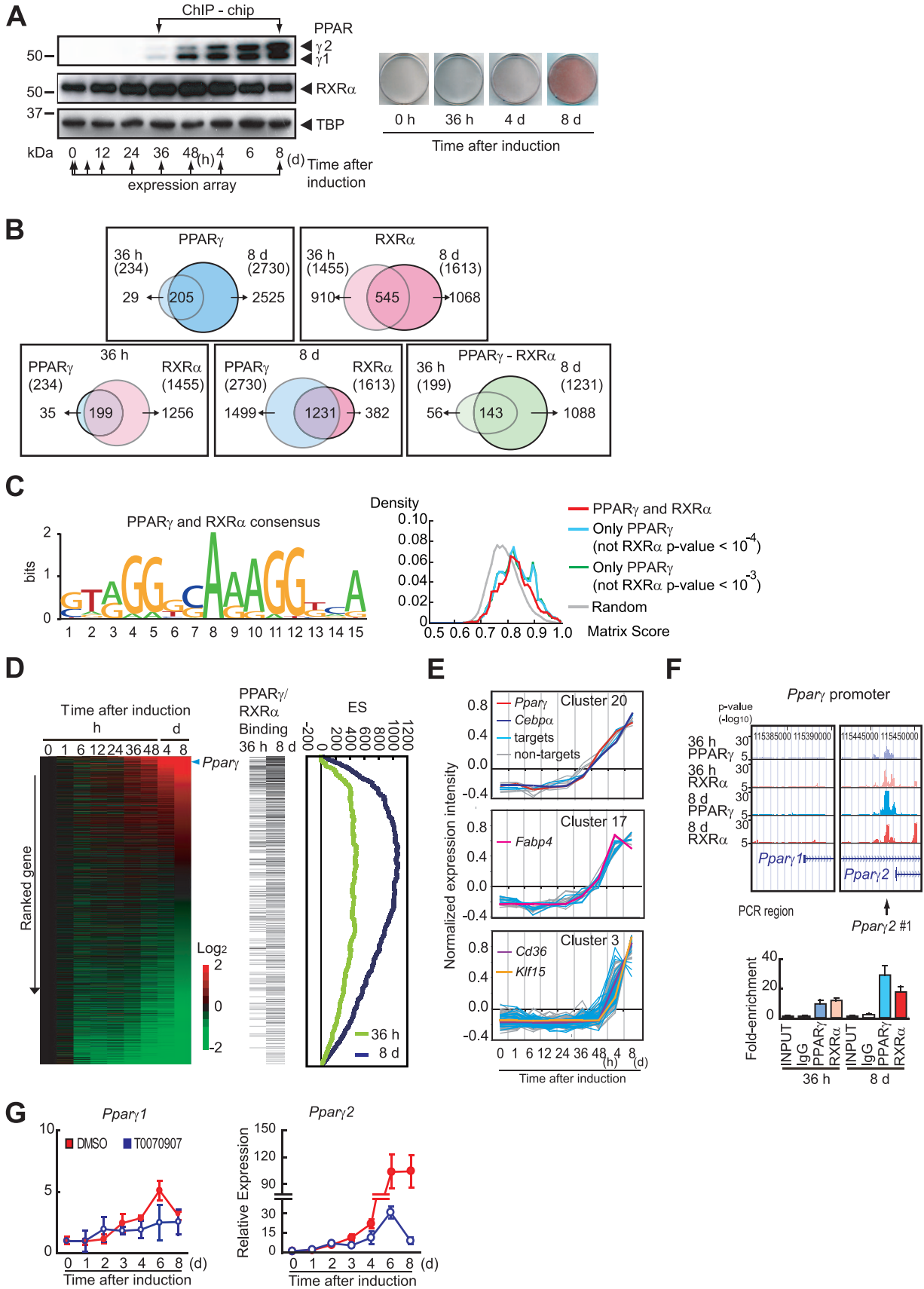
Cell fractionation and immunoblot analysis. Whole-cell extracts were separated into the soluble supernatant and the chromatin-containing fraction as described previously (34). The isolation and immunoblot analysis of the nuclear extracts were performed as described previously (26).

RESULTS

Identification of PPAR γ binding sites by ChIP-chip analysis. To reveal PPAR γ -dependent transcriptional programs during adipocyte differentiation, we performed global gene expression and ChIP-chip analysis. 3T3-L1 preadipocytes were induced to differentiate through conventional cocktails containing MDI. Figure 1A shows an immunoblot analysis of the nuclear extracts from cells at the indicated time of differentiation (left panel). PPAR γ is expressed beginning at 36 h and is robustly induced by day 8 of differentiation. A global gene expression analysis was performed at the indicated times, and the data were combined with the ChIP-chip data (see below). ORO staining shows that a substantial amount of lipid accumulates in 3T3-L1 cells (right panel).

A ChIP-chip analysis of the 3T3-L1 cells was conducted at 36 h and at day 8 of differentiation using a promoter array platform, which contains 28,000 mouse proximal promoter sequences, typically located between -6.0 to $+2.5$ kb relative to the transcription initiation site. Triplicate ChIPs were performed using a newly generated monoclonal antibody against PPAR γ . Our analysis identified highly significant PPAR γ binding ($a P$ value of $<10^{-4}$ at a false discovery rate of <0.1) at 234 sites at 36 h of differentiation (Fig. 1B, top left panel; see also Table S1 in the supplemental material) and 2,730 sites on day 8. The number of sites to which PPAR γ bound increased dramatically in correlation with a robust increase in PPAR γ expression. Of the promoters occupied by PPAR γ at 36 h of differentiation, 88% (205/234) were also occupied on day 8 of differentiation.

Identification of RXR α binding sites by ChIP-chip analysis. PPAR γ is known to bind to direct repeat 1 (DR1) as a heterodimer with RXR α to exert its transcriptional activity (10). We next undertook the identification of the RXR α direct target genes by ChIP-chip using a newly generated monoclonal antibody against RXR α that does not cross-react with other RXR family members (i.e., RXR β and RXR γ) (see Fig. S1 in the supplemental material). This analysis identified 1,455 occupied sites at 36 h of differentiation, 1,613 sites at day 8 of differentiation ($P < 10^{-4}$; false discovery rate, <0.1), and 545 sites that were common to both (Fig. 1B, top right panel). These data indicate that RXR α targets distinct but overlapping



repertoires of promoters between the early (36 h) and late (day 8) differentiation of 3T3-L1 cells.

PPAR γ and RXR α target the same repertoire of promoters.

Independent ChIP-chip analyses with antibodies to PPAR γ and RXR α revealed significant overlap between PPAR γ and RXR α target promoters in 3T3-L1 cells. The results indicate that endogenous PPAR γ and RXR α in fact bind to the same repertoire of binding sites in 3T3-L1 cells in early differentiation (Fig. 1B, bottom panels).

An analysis of the regions identified as common PPAR γ and RXR α targets by ChIP-chip demonstrated a distinctive DNA binding sequence, 5'-(A/G)GG(T/G)CA (A/G) AGG(T/G)CA-3', that corresponds to DR1 (5'-AGGTCA A AGGTC A-3') (10) (Fig. 1C, left panel). Furthermore, the 1,499 sites occupied by PPAR γ but not by RXR α , showed significant enrichment of this DR1 motif compared to that of randomly selected genomic sequences ($P < 10^{-57}$ by t test) (Fig. 1C, right panel). Similar results were obtained when a comparison was made at the less-stringent threshold of the RXR α P value of $<10^{-3}$ (Fig. 1C, right panel). These data strongly support the hypothesis that PPAR γ forms heterodimers with other members of the RXR family in differentiation. The overall picture from these studies is largely consistent with other recent reports (14, 22).

Identification of PPAR γ and RXR α target genes. A functional annotation of genes with PPAR γ binding revealed that PPAR γ binds to a wide assortment of genes involved in cellular metabolism (see Table S1 and S2 in the supplemental material). The functions of a large number of target genes are

consistent with the role of PPAR γ in the regulation of adipogenesis and lipid storage. These products of target genes include proteins involved in lipid and glucose metabolism, adipocytokines, cellular process proteins, apoptotic machinery proteins, intracellular signaling cascade proteins, transcription factors, and enzymes of histone modification. These include a well-characterized pro- or antiadipogenic factor, Nr2f2 (COUP-TFII) (35), Klf15 (20), and, importantly, PPAR γ 2. PPAR γ was also found to bind to genes that encode SET domain proteins, which are histone-modification enzymes.

PPAR γ directly regulates PPAR γ 2 gene expression. To determine whether promoter occupancy by PPAR γ and RXR α correlates with transcriptional changes of the targeted genes, we combined ChIP-chip results with gene expression profiling data on differentiating 3T3-L1 cell lines. GSEA (19, 27) was used to test whether the enrichment of a PPAR γ /RXR α heterodimer binding genes occurred in either the upregulated or downregulated genes. This analysis revealed that of the genes induced at day 8 of differentiation, those bound by both PPAR γ and RXR α showed a significant enrichment ($P < 10^{-6}$, both at 36 h and day 8) (Fig. 1D). Figure S2 in the supplemental material presents target genes in the network-based clustering of coexpressed genes across the entire time course of differentiation. Figure 1E shows examples of three individual clusters. ChIP-chip and ChIP-qPCR analyses demonstrated that the *Ppar γ 2* gene showed significant promoter binding by the PPAR γ /RXR α heterodimer at both 36 h and day 8 of differentiation (Fig. 1F). These data suggest that PPAR γ drives PPAR γ 2-mediated transcription. To test this

FIG. 1. Genome-wide promoter occupancy of PPAR γ and RXR α in 3T3-L1 adipocytes. (A) Experimental design for transcriptome and ChIP-chip analyses. Postconfluent 3T3-L1 cells were induced to differentiate as described in Materials and Methods. Cells were harvested at the indicated times, and nuclear extracts were prepared. PPAR γ protein expression throughout the adipocyte differentiation of 3T3-L1 cells (left panel) and ORO staining (right panel) are shown. Nuclear extracts were subjected to immunoblot analysis using anti-PPAR γ antibody (IgG-A3409) and RXR α (IgG-K8508) (left panel). ORO staining was performed at several time points (right panel). The expression of $\sim 39,000$ transcripts at the time points indicated by arrows was measured using an Affymetrix Mouse Genome 430 2.0 array and applied to ChIP-chip data (see Fig. S2 in the supplemental material). (B) Venn diagrams illustrating the overlap of either PPAR γ or RXR α binding sites at 36 h and at day 8 (top left and top right panels, respectively), the overlap in PPAR γ and RXR α binding sites at either 36 h or day 8 (bottom left and bottom middle panels, respectively), and the overlap of both PPAR γ and RXR α at 36 h and at day 8 (bottom right panel) obtained by ChIP-chip analyses using anti-PPAR γ antibodies (both IgG-A3409 and sc-7273 together) or anti-RXR α antibody (IgG-K8508). (C) Identification of enriched motifs in the PPAR γ and RXR α binding sequences in 3T3-L1 cells (left panel). The height of each letter represents the relative frequency of nucleotides at different positions in the consensus. The motif score distribution for 2,730 PPAR γ binding sites at day 8 is shown (right panel). The "PPAR γ and RXR α " line (red) corresponds to the 1,231 sites that both PPAR γ and RXR α bound, and the "Only PPAR γ (not RXR α p-value $< 10^{-4}$)" line (light blue) corresponds to the rest of the 1,499 sites. The "Only PPAR γ (not RXR α p-value $< 10^{-3}$)" line (green) corresponds to the less-stringent threshold for RXR α . The "Random" line (gray) shows the average of 1,000 randomly selected genomic regions. (D) Graphic representation of GSEA enrichment scores (ES) and distribution of the PPAR γ and RXR α co-occupied genes along the transcripts from the complete time course of 3T3-L1 adipocyte differentiation. Gene expression data from the complete time course of 3T3-L1 adipocyte differentiation are illustrated by heat map. Data measurements are presented relative to time zero. The probes were sorted by the ratio at day 8 (ranked gene list). Increased or decreased mRNA expression is represented by red or green (left panel). Increasing green intensity denotes genes that decrease in expression with respect to time zero, and increasing red intensity denotes genes that increase in expression with respect to time zero. The horizontal thin bar indicates the probe of each gene bound by both PPAR γ and RXR α at either 36 h or day 8 of differentiation (middle panel). For each gene set, the ES calculated by GSEA were drawn (right panel). The running sum from the top of the ranked gene list was plotted. If the PPAR γ /RXR α binding genes were found frequently from the top, the sum increases and vice versa. High ES (maximum of the running sums) means that these genes are enriched in the top of the distribution. (E) Time course of gene expression in the early (cluster 20 and 17) and late (cluster 3) response clusters. PPAR γ -bound genes are shown in light blue, and non-PPAR γ binding genes in gray. *Ppar γ* , *Fabp4*, *Klf15*, *Cd36* (detected as a PPAR γ -bound gene), and *Cebp α* (not detected as a PPAR γ -binding gene) are also shown in the indicated colors. (F) PPAR γ and RXR α binding to the *Ppar γ 2* promoter as demonstrated by ChIP-chip analysis (top right panel) and ChIP-qPCR with *Ppar γ 2* promoter-specific primers that amplifies the PCR region *Ppar γ 2 #1* (bottom panel). ChIP-chip data representing the enrichment ratio of ChIP versus input DNA hybridization intensity are shown as P values ($-\log_{10}$). Arrow below the top right panel denotes the region of the sets of primers used for the ChIP-qPCR in the bottom panel. (G) Inhibition of PPAR γ activity blocks the induction of PPAR γ 2. Two days postconfluence, 3T3-L1 cells were induced to differentiate in the presence or absence of 20 μ M T0070907 (PPAR γ antagonist) (Cayman Chemical) and harvested at the indicated times. The mRNA levels of *Ppar γ 1* and *Ppar γ 2* were analyzed by qRT-PCR using specific primers. The mRNA levels were normalized to those of *Ppib*. Results are expressed as means \pm standard deviations.

hypothesis, we treated 3T3-L1 preadipocytes with T0070907 (a selective antagonist of PPAR γ) following the induction of differentiation by MDI and examined the mRNA levels of each PPAR γ isoform by quantitative reverse transcriptase PCR (qRT-PCR) analyses with primer sets that discriminate between PPAR γ 1 and PPAR γ 2. Consistently with previous results by Zuo et al. (37), PPAR γ 1 mRNA levels increased by three- to fivefold and were not significantly altered by treatment with T0070907 during differentiation (Fig. 1G, left panel). PPAR γ 2 mRNA levels were increased dramatically at day 4 of differentiation, and this increase was almost completely blunted by T0070907 treatment (Fig. 1G, right panel). The data above demonstrated that PPAR γ drives PPAR γ 2-mediated transcription, thereby promoting adipogenesis in 3T3-L1 cells.

PPAR γ controls the transcription of several SET domain protein genes. The modification of histones, especially by lysine methylation, plays a pivotal role in a wide range of cellular processes, including heterochromatin formation and transcriptional regulation. The methylation of histones at lysine residues is catalyzed by the conserved SET domain family proteins. Our CHIP-chip data showed that PPAR γ targets several genes that encode SET domain proteins. This suggests that PPAR γ may also contribute to histone modification through the transcriptional regulation of SET domain proteins.

To test this hypothesis, we searched databases for genes that encode SET domain proteins and found that the mouse genome encodes at least 45 SET domain proteins. We then examined CHIP-chip and gene expression data for these genes throughout adipocyte differentiation. Of these 45 genes, 28 genes were expressed in 3T3-L1 cells at some time during differentiation (here, an "expressed" gene is defined as a transcript with a detection call of "present" across all time points as well as one with an average difference call above 100 for at least one time point across the experimental time points). CHIP-chip identified highly significant PPAR γ binding to 10 of the 45 genes ($P = 2.3 \times 10^{-8}$), and 8 of these were expressed (the *Ehmt1*, *Ehmt2* [also known as G9a histone methyltransferase], *Ezh2*, *Setd5*, *PR-Set7/Setd8* [*Setd8*], *Setdb1*, *Suv39h1*, and *Wbp7* genes) (Fig. 2A and B; see also Table S1 and the experimental procedures in the supplemental material).

Furthermore, the siRNA-mediated knockdown of PPAR γ and/or the pharmacological inactivation of PPAR γ by treatment with an antagonist blunted the altered expression of six of these genes (the *Setdb1*, *Setd5*, *Setd8*, *Ezh2*, *Suv39h1*, and *Wbp7* genes). Three of these (the *Setdb1*, *Setd5*, and *Setd8* genes) showed a complete loss of regulation (Fig. 2C). Figure 2D shows that *Ppar γ* gene expression and the subsequent lipid accumulation were indeed abolished by the transfection of siRNA specific to PPAR γ . These data strongly suggest that PPAR γ binding to genes that encode SET domain proteins leads to the transcriptional regulation of gene expression and further suggests the involvement of PPAR γ in epigenetic changes during adipocyte differentiation.

Setdb1 and Setd8 are critical regulators of 3T3-L1 adipocyte differentiation. If this is true, the alteration of their expressions should modulate adipogenesis. To test this hypothesis, we used an siRNA approach to knock down the expression of *Setdb1* and *Setd8*. Because the biochemical function of *Setd5* has not been reported, we focused on *Setdb1* and *Setd8*. Two indepen-

dent, efficacious siRNA oligonucleotide sequences from each of the *Setdb1* and *Setd8* genes were transfected into 3T3-L1 cells. These cells were cultured to confluence and exposed to DEX alone or to the adipogenic MDI cocktail.

Because the MDI cocktail is very efficient in converting 3T3-L1 preadipocytes into mature adipocytes, we reasoned that it would be difficult to assess an increase in adipogenesis using MDI. Therefore, we only used DEX treatment to induce differentiation, which is much more inefficient at inducing differentiation than the complete cocktail. ORO staining revealed that cells transfected with *Setdb1* siRNA accumulated significantly more lipid than the negative control siRNA-transfected cells (Fig. 3A). Among the upregulated adipogenic genes identified by the global gene expression profiling of *Setdb1* knockdown cells were PPAR γ and C/EBP α together with many PPAR γ target genes including the *Fabp4*, *Cd36*, and *AdipoQ* genes. By contrast, the expression of other transcription factors involved in adipogenesis did not change in response to *Setdb1* depletion (Fig. 3B).

In comparison when exposed to MDI, cells transfected with siRNA for *Setd8* showed decreased lipid accumulation relative to siRNA negative control transfected cells (Fig. 3C). The expressions of PPAR γ and C/EBP α were reduced in *Setd8* knockdown cells induced to differentiate by MDI. This was accompanied by the decreased expression of PPAR γ targets. Other adipogenic factors such as C/EBP β or δ did not change significantly (Fig. 3D). These results demonstrate that the knockdown of *Setdb1* promotes adipogenesis, whereas the upregulation of *Setd8* is necessary for the normal differentiation of 3T3-L1 cells.

Setdb1 and Setd8 levels are altered in mouse models of obesity. To examine if these SET domain proteins show altered expression in mouse models of obesity, we examined adipose tissue from two different mouse models of obesity, one that occurs as a result of the high-fat feeding of the C57BL/6J mouse (DIO) and the other is the genetically predisposed obese *ob/ob* mouse. For DIO, we randomized 6-week-old C57BL/6J littermates and fed them either normal or high-fat chow for 8 weeks, extracted RNA from epididymal fat depots, and examined the expression of *Setdb1* and *Setd8* by qRT-PCR. We found that DIO significantly decreased mRNA levels for *Setdb1* and increased *Setd8* levels in white adipose tissue (Fig. 3E, left panels). A similar downregulation of *Setdb1* and upregulation of *Setd8* expression was observed in adipose tissues from 10-week-old *ob/ob* genetically obese mice compared to that of matched controls (Fig. 3E, right panels).

Setd8 is a bona fide PPAR γ target gene. We asked whether the PPAR γ /RXR α heterodimer directly activates the *Setd8* promoter. A DNA fragment containing the 5' flanking region of the mouse *Setd8* gene was subcloned into the promoterless luciferase reporter gene pGL3 basic and transiently transfected into 3T3-L1 cells along with the PPAR γ and RXR α expression plasmids. As shown in Fig. 4A, the expression levels of luciferase were increased fivefold. Importantly, the deletion of the PPAR γ /RXR α binding sites identified in our CHIP-chip analysis abolished promoter activity. CHIP-qPCR confirmed that the *Setd8* promoter fragment from the -500-bp region was enriched by the PPAR γ antibody (Fig. 4B). In addition, the ectopic expression of PPAR γ by retroviral transduction increased the expression of

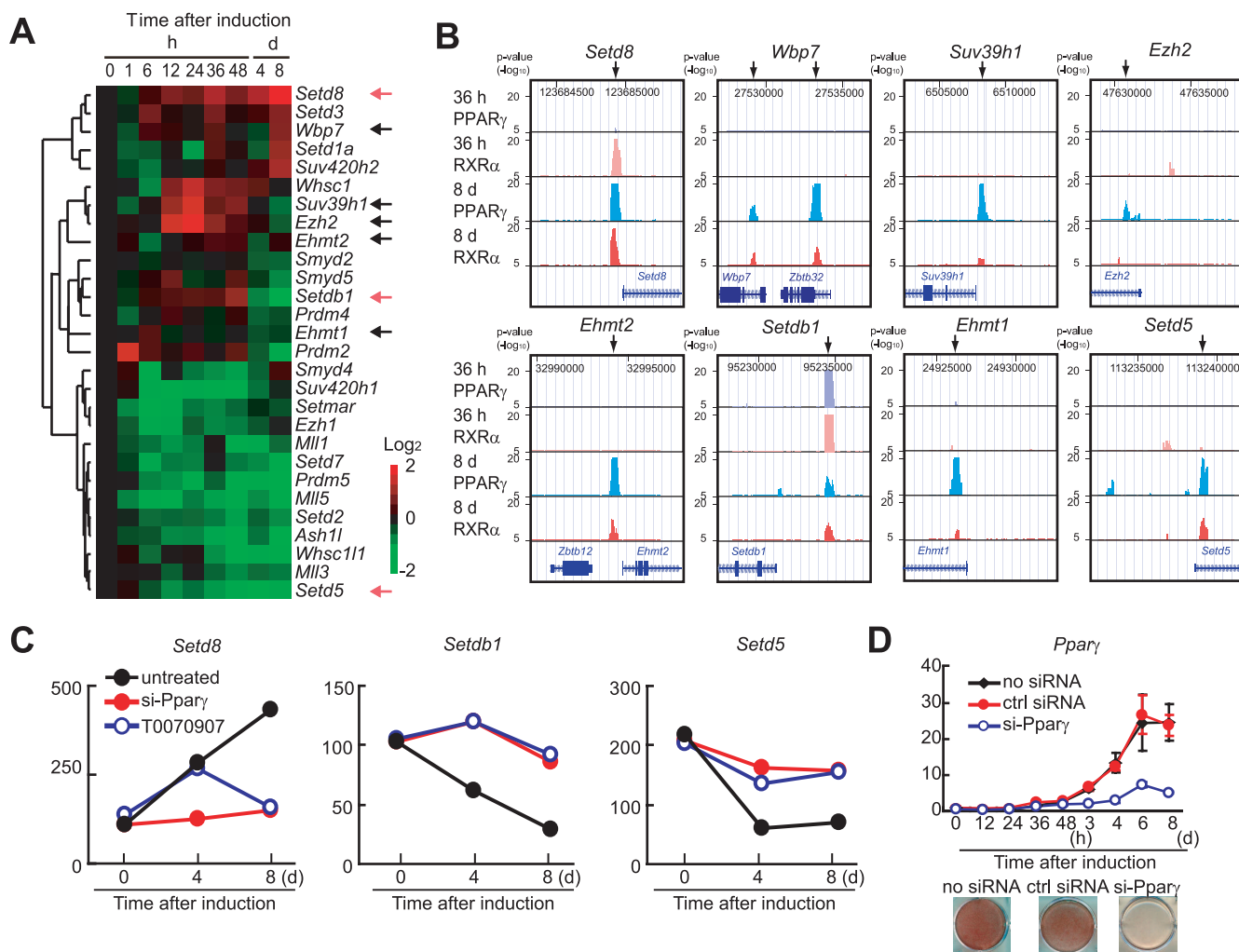


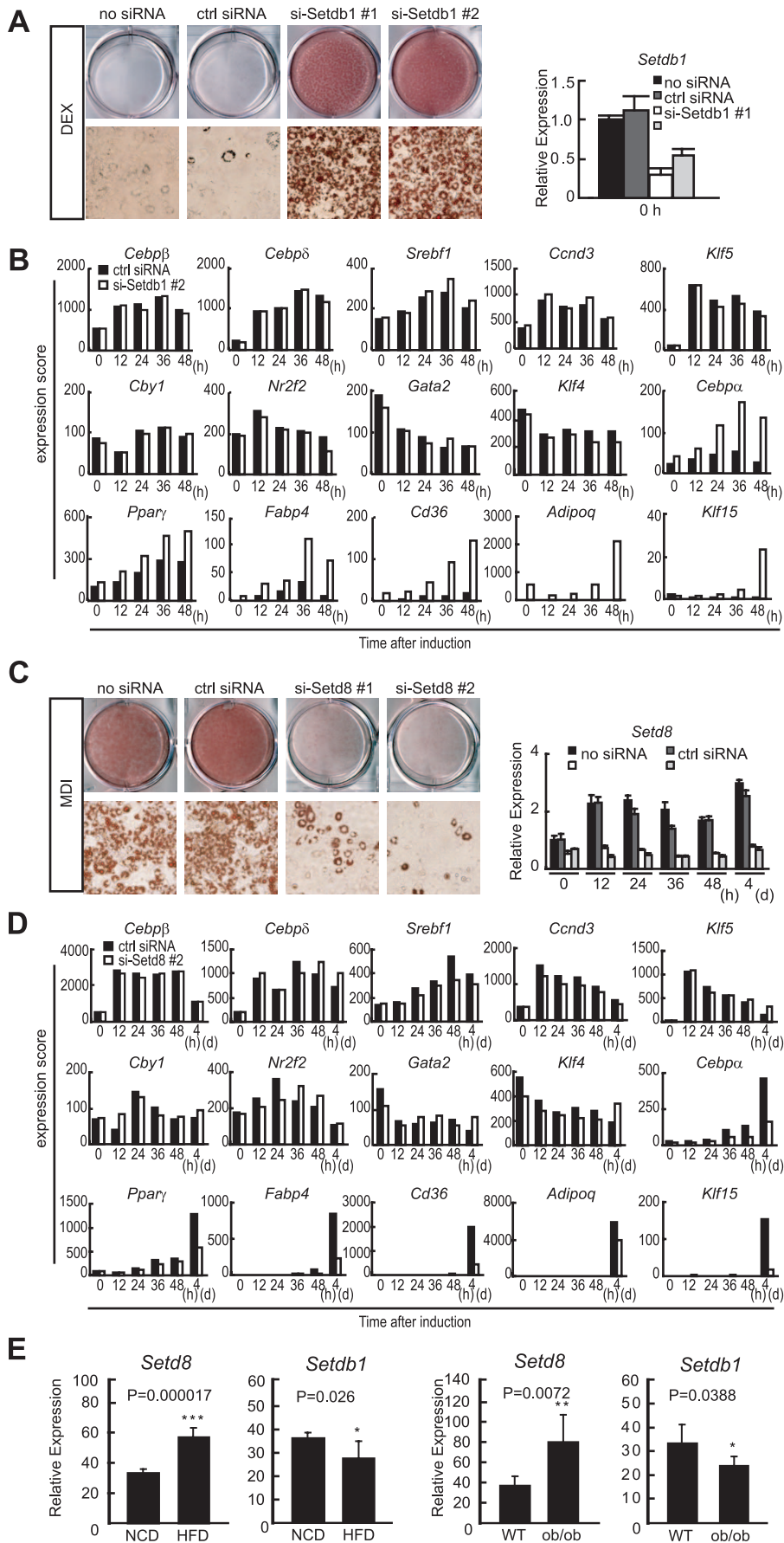
FIG. 2. PPAR γ binds to several genes that encode SET domain proteins. (A) Microarray heat map depicting expression changes of SET domain protein genes from the complete time course of 3T3-L1 adipocyte differentiation. Arrows denote genes bound by PPAR γ . (B) ChIP-chip analysis revealed that PPAR γ binds to several SET domain proteins. (C) Transcriptional changes induced by siRNA-mediated depletion of PPAR γ and pharmacological inactivation of PPAR γ . Transcriptional analyses were carried out using microarray analysis software provided by Affymetrix, and significantly increased or decreased genes were shown. Transcript levels were compared to the levels in untreated cells versus either si-Ppar γ -transfected or T007097-treated 3T3-L1 cells harvested at the indicated time. (D) 3T3-L1 cells were untreated (no siRNA) or treated with PPAR γ -specific siRNA (si-Ppar γ) or the siRNA negative control (ctrl siRNA) prior to the induction of differentiation as described. Cells at the indicated times of differentiation were harvested for isolation of total RNA, and PPAR γ mRNA levels were quantified by qRT-PCR (top panel). ORO staining was performed on day 8 (bottom panel).

Setd8 (Fig. 4C). Taken together, these results all demonstrated that Setd8 is a bona fide target of PPAR γ .

H4K20me1 levels are robustly increased during adipocyte differentiation. As shown in Fig. 2C, Setd8 mRNA levels increase robustly in correlation with PPAR γ expression during differentiation. This is consistent with our identification of Setd8 as a direct target of PPAR γ . We hypothesized that the total abundance of H4K20me1 in 3T3-L1 cells also increased in correlation with Setd8 expression. Intriguingly, an immunoblot analysis demonstrated that H4K20me1 levels in 3T3-L1 cells are substantially increased during differentiation (Fig. 4D).

H4K20me1 histone modification enhances gene expression. To further examine if the increased total amount of H4K20me1 levels contributes to the number of genes modified

by H4K20me1, we performed high-resolution ChIP-seq with an antibody that detects H4K20me1 at day 0 and day 8 of differentiation. This analysis using the stringent cutoffs of enrichment of H4K20me1 count over the input/estimate count (fivefold or more) revealed that the numbers of H4K20me1-modified genes are profoundly increased: 1,854 genes at day 0 and 4,012 genes at day 8 (Fig. 4E). The combination of H4K20me1 ChIP-seq and global gene expression profiling also demonstrated that more than 85% of the genes modified by H4K20me1 are expressed at a higher level compared to those that are not modified by H4K20me1 (Fig. 4F). In addition, expression changes are also correlated with the H4K20me1 modification ratio during differentiation (Fig. 4G). These data



indicate that H4K20me1 modification enhances gene expression in 3T3-L1 cells.

Increased H4K20me1 in PPAR γ and its target genes during adipogenesis. We next examined the level of H4K20me1 modification of PPAR γ target genes. Of the 708 “present” genes occupied by PPAR γ at day 8, 383 genes (54%) were modified by H4K20me1 (Fig. 4H, top panel). Of these 383 occupied by the PPAR γ /RXR α heterodimer that are modified by H4K20me1, 204 genes (53%) were upregulated (1.5-fold or more), 102 genes (27%) hardly changed in expression (upregulated or downregulated less than 1.5-fold), and only 77 genes (20%) were downregulated (1.5-fold or less). Of the 204 genes that were upregulated, 150 genes (74%) are newly modified by H4K20me1; these genes include the PPAR γ gene and many of the PPAR γ targets involved in adipogenesis (Fig. 4H, bottom panel; see also Table S3 in the supplemental material).

Setd8 regulates the expression of PPAR γ and its targets through H4K20 monomethylation. We identified H4K20me1 modifications to sites downstream of the transcription start sites (i.e., gene body) for both PPAR γ 1 and PPAR γ 2 and their targets, including *Fabp4* and *Cd36*, at day 8 (Fig. 5A). The validation of H4K20me1 modification by ChIP-qPCR analysis showed that these genes were indeed modified by H4K20me1 at day 8 (Fig. 5B).

We next tested if Setd8 mediates the H4K20 monomethylation of chromatin associated with PPAR γ and/or its adipogenic targets. We used a ChIP assay to measure the level of H4K20me1 in 3T3-L1 cells treated with siRNA specific to Setd8 or control siRNA. Importantly, H4K20me1 levels at PPAR γ 1 and PPAR γ 2 and their adipogenic target genes were markedly decreased upon Setd8 depletion, indicating the specific role of Setd8 in the H4K20me1 chromatin modification of these genes (Fig. 5C). The immunoblot in the inset of Fig. 5C shows that Setd8 levels were reduced in the Setd8-specific siRNA transected cells and that the expression of H4K20me1 was also decreased in correlation with the Setd8 level.

H4K20me1 modification levels at PPAR γ target genes are correlative to PPAR γ transcriptional activity. H4K20me1 modification of the *Ppar γ* gene and its targets was increased by treatment with troglitazone and profoundly reduced with PPAR γ antagonist (Fig. 5D). These data show that the activation of PPAR γ transcriptional activity leads to the induction of H4K20me1 modification at PPAR γ and its targets and subse-

quent adipogenesis. Finally, to assess the epistatic relationship between Setd8 and PPAR γ in adipogenesis, we determined the effect of the ectopic expression of this protein on adipocyte differentiation in NIH 3T3 cells, which are not committed to the adipocyte fate (4). We infected NIH 3T3 cells transduced with PPAR γ 2 with retrovirus for Setd8 and tested whether they exhibited enhanced differentiation. After stable selection, cells were induced to differentiate by treatment with the standard MDI adipogenic cocktail or with troglitazone for 2 days. Cells expressing both Setd8 and PPAR γ 2 accumulated significantly more lipid than cells expressing PPAR γ 2 alone under both conditions (Fig. 5E). Altogether these data demonstrate that Setd8 regulates the expression of PPAR γ and its targets through H4K20 monomethylation to enhance adipocyte differentiation.

DISCUSSION

The methylation of lysine residues in histones is an important epigenetic event that correlates with functionally distinct regions of chromatin. In the current study, by combining global gene expression analyses with a ChIP-chip approach, we report that two well-characterized HKMTs, Setdb1 and Setd8, are coordinately regulated by PPAR γ and their expression leads to adipocyte differentiation through chromatin modifications.

The knockdown of these SET domain proteins demonstrated that they are indeed involved in adipogenesis. mRNA levels for Setdb1 decreased in concert with adipocyte differentiation. The knockdown of Setdb1 resulted in the stimulation of adipogenesis even when isobutylmethylxanthine and insulin were omitted from the differentiation cocktail. By contrast, Setd8 mRNA was increased in abundance throughout adipocyte differentiation and the knockdown of Setd8-impaired adipocyte differentiation (Fig. 3A and C). In this context, Setdb1 acts as an antiadipogenic factor and Setd8 acts as proadipogenic factor, and it is reasonable to think that Setdb1 is downregulated and Setd8 is upregulated during adipocyte differentiation. It remains to be determined whether Setdb1 is directly downregulated by PPAR γ . PPAR γ may contribute to the transcriptional regulation of Setdb1 and thereby regulate trimethylated H3K9, a silencing histone marker, to promote differentiations as reported (28). We find that Setd8 is a bona fide PPAR γ target (Fig. 4). PPAR γ upregulates Setd8 and thereby

FIG. 3. Effect of the siRNA knockdown of Setdb1 and Setd8 on 3T3-L1 adipogenesis. 3T3-L1 cells were transfected with siRNAs for Setdb1 (si-Setdb1#1 and #2) (5 nM) or Setd8 (si-Setd8#1 and #2) (20 nM) or the siRNA negative control (ctrl siRNA). (A and B) siRNA-mediated knockdown of Setdb1 promotes 3T3-L1 adipogenesis. Cells were induced to differentiate by DEX alone. (A) ORO staining performed at day 8 (left panel). The mRNA levels of Setdb1 after the knockdown of Setdb1 was quantified by qRT-PCR. The data are the averages of three replicates, and the error bars represent the standard deviations (right panel). (B) Transcriptional changes of adipogenic genes in Setdb1 knockdown cells. Cells were harvested at the indicated time of differentiation, and transcriptional analyses were carried out using a microarray. (C and D) siRNA-mediated knockdown of Setd8 inhibits 3T3-L1 adipogenesis. Cells were induced to differentiate by treatment with the MDI cocktail. (C) ORO staining was performed at day 8 (left panel). The mRNA level of Setd8 after the knockdown of Setd8 was quantified by qRT-PCR. The data are the averages of three replicates, and the error bars represent the standard deviations (right panel). (D) Transcriptional changes of adipogenic genes in Setd8 knockdown cells. Cells were harvested at the indicated times of differentiation, and transcriptional analyses were carried out using a microarray. (E) Setdb1 and Setd8 are expressed in the white adipose tissue of mice and regulated by obesity (left panels). Matched littermates were fed for 3 months with a normal (NCD) or high-fat chow diet (HFD) (DIO), and adipose depot gene expression was analyzed with real-time PCR, which demonstrated a statistically significant decrease in Setdb1 expression and an increase in Setd8 in DIO adipose tissue ($n = 6$) (right panels). Setdb1 expression levels are reduced in genetically obese (*ob/ob*) fat depots compared to those of the controls ($n = 6$). *Ppib* serves as a loading control for qRT-PCR. *, $P < 0.05$. The animals and diet conditions are described in the supplemental material experimental procedures.

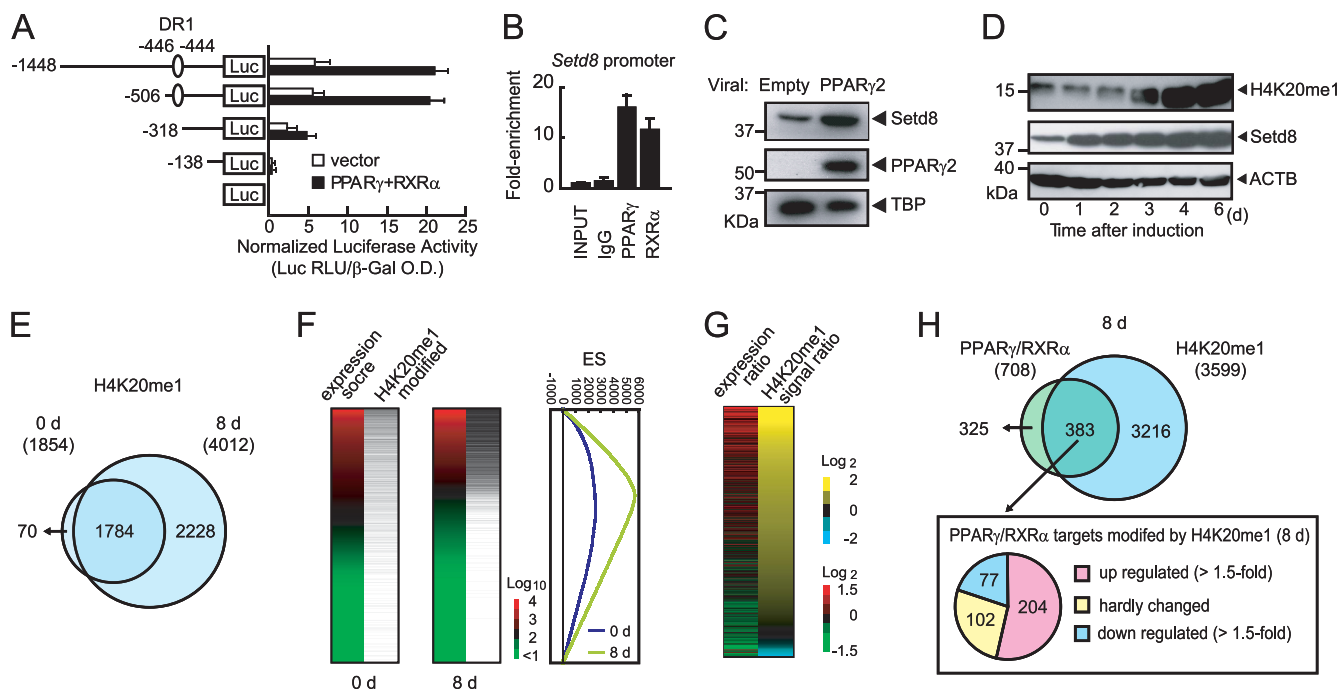


FIG. 4. PPAR γ directly regulates *Setd8* expression and increases H4K20me1 in 3T3-L1 cells during differentiation. (A) 3T3-L1 cells were transfected with pGL3-*Setd8*, a luciferase reporter construct under the control of the *Setd8* promoter (–1458 to –1), or with unilateral deletion constructs that lack potential PPAR γ /RXR α heterodimer binding sites. For each construct, we cotransfected a construct expressing β -galactosidase driven by a cytomegalovirus promoter to serve as an internal control. Each value represents the mean of duplicate experiments. Error bars indicate the range of the duplicates. (B) ChIP-qPCR analyses of PPAR γ and RXR α recruitment on *Setd8* promoter in 3T3-L1 cells at day 8 of differentiation. The data are the average of three replicates, and error bars represent the standard deviations. (C) Upregulation of *Setd8* protein in NIH 3T3 cells transduced with retrovirus carrying PPAR γ 2. NIH 3T3 cells were infected carrying cDNA for PPAR γ or empty vector. The expressions of *Setd8* and PPAR γ were assessed by immunoblot analysis using anti-*Setd8* (sc-54996) and anti-PPAR γ (IgG-A3409). Equal loading of the proteins was confirmed by the detection of nuclear protein TBP (NB500-700). (D) Immunoblot analysis showing the upregulation of *Setd8* during adipogenesis. 3T3-L1 cells were induced for differentiation with MDI and harvested at the indicated times for whole-cell lysate. Protein expressions were assessed using anti-*Setd8* (sc-54996) and anti-H4K20me1 (07-440). Equal loading of the proteins was confirmed by the detection of β -actin (ACTB; A5441). (E) Venn diagram illustrating the overlap of H4K20me1 genes before differentiation (0 d) or at day 8 (8 d) of differentiation obtained by ChIP-seq using anti-H4K20me1 (ab9051). (F) H4K20me1 modification is correlated with gene expression. Gene expressions of 3T3-L1 cells at day 0 (left panel) or day 8 (middle panel) are illustrated by heat map. The genes were sorted by the mRNA expression score. mRNA expression is represented by red (high expression) or green (low expression). For reference, a color intensity scale is included at the right side. The black bar indicates the genes modified by H4K20me1. The horizontal thin bar indicates each gene modified by H4K20me1 before (0 d) or on day 8 of differentiation (left and middle panels). For each gene set, the enrichment scores calculated by GSEA were drawn (right panel). (G) The H4K20me1 modification level is correlated with the gene expression level. The gene expression ratio (day 8/day 0; left) and H4K20me1 modification ratio (right) are illustrated. Each gene (denoted by a horizontal thin line) was sorted by H4K20me1 expression ratio. (H) Top panel, Venn diagram illustrating the overlap of PPAR γ /RXR α target genes and H4K20me1-modified genes at day 8. Bottom panel, the pie graph shows the number of genes of PPAR γ /RXR α targets that are also modified by H4K20me1.

regulates H4K20me1 to induce PPAR γ and its targets to acquire the adipocyte phenotype. Intriguingly, *Setdb1* and *Setd8* are expressed in adipose tissues and reciprocally expressed in rodent models of obesity; the downregulation of *Setdb1* and upregulation of *Setd8* (Fig. 3E) suggest that these proteins play a role in regulating adiposity in the excess energy state.

Most intriguingly, H4K20me1 levels are robustly induced toward the end of differentiation (Fig. 4D), and this is accompanied by increased numbers of genes modified by H4K20me1. In addition, H4K20me1 modification levels at PPAR γ target genes are correlative to PPAR γ transcriptional activity (Fig. 5D). A combination of H4K20me1 ChIP-seq and transcriptome analyses demonstrated that more than 85% of genes modified by H4K20me1 are expressed at high levels, suggesting a role for activating histone chromatin modification. This is also supported by the recent ChIP analyses demonstrating a

preferential association of H4K20me1 with selected transcriptionally active or competent genes (29, 33).

Although the PPAR γ 1 gene is not modified by H4K20me1 before differentiation (Fig. 5A and B), an appreciable amount of PPAR γ 1 mRNA is detected (Fig. 1G). Toward the end of differentiation, PPAR γ 1 gene expression levels increase by four- to fivefold in correlation with the modification by H4K20me1 (Fig. 1G and 5B). Therefore, we postulate that H4K20me1 functions to enhance gene transcription rather than initiation. H4K20me1 may contribute to the robust gene expression required to progress to the adipocyte phenotype. Recent ChIP sequencing assays also revealed strong evidence that H4K20me1 is associated predominantly in transcript elongation rather than the initiation of transcription (1).

Our data demonstrate that PPAR γ is required for *Ppar γ 2* gene expression. PPAR γ /RXR α heterodimers bind directly to

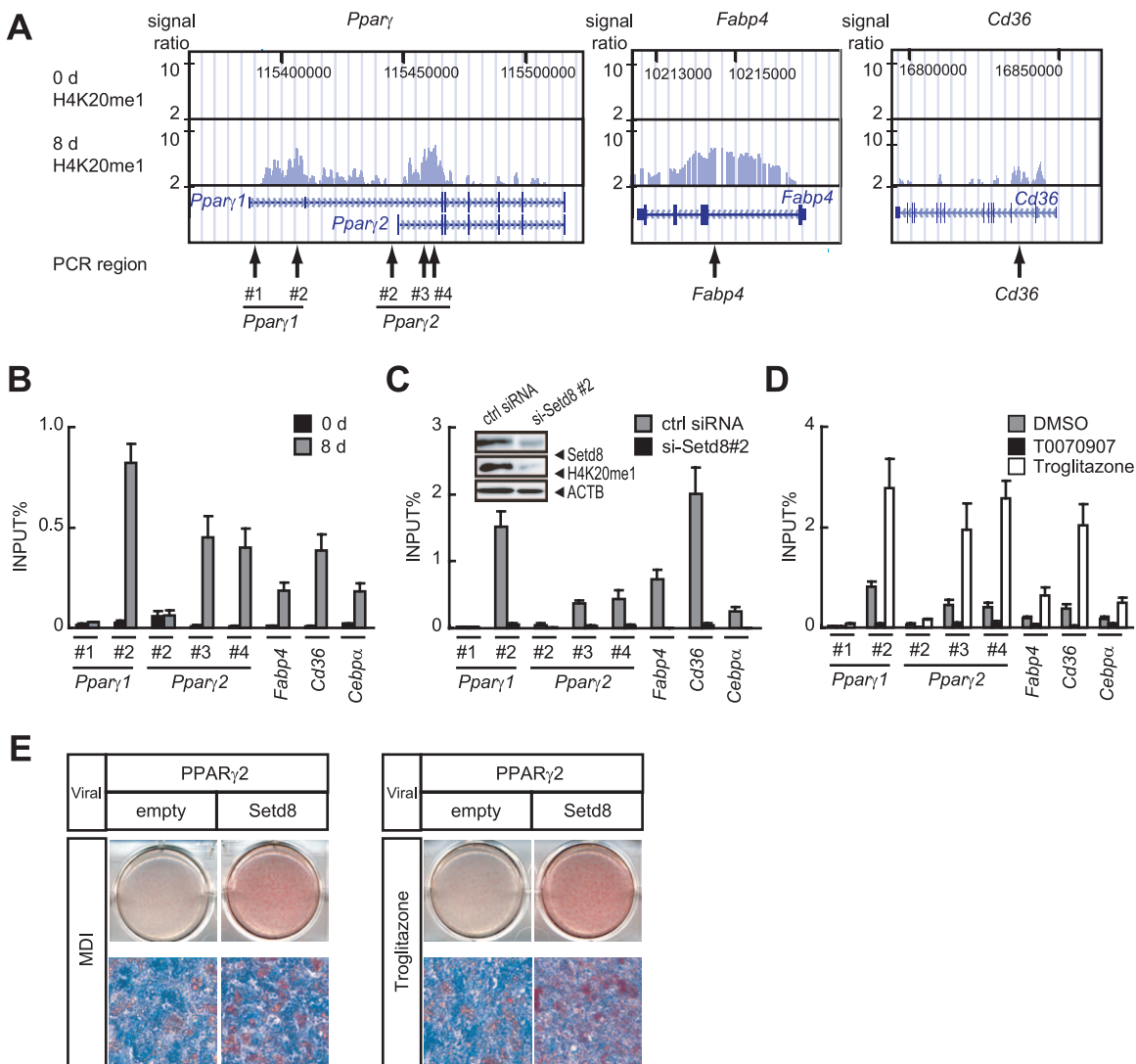


FIG. 5. Setd8 regulates the expression of PPAR γ and its targets through H4K20 monomethylation. (A and B) ChIP-seq of the *Ppar γ 1*, *Ppar γ 2*, *Fabp4*, and *Cd36* genes (A) and ChIP-qPCR analyses of H4K20me1 modifications on the *Ppar γ 1*, *Ppar γ 2*, *Fabp4*, *Cd36*, and *Cebp α* genes in 3T3-L1 preadipocytes (0 d) and adipocytes (8 d). (B) The arrows in panel A denote the regions of the sets of primers used for the ChIP-qPCR. (C) 3T3-L1 cells transfected with siRNA specific to Setd8 (si-Setd8 #2) or control siRNA (ctrl siRNA) were induced for differentiation and analyzed for H4K20me1 modifications by ChIP-qPCR using the specific primers as shown in panel A. Inset, the cells at day 4 of differentiation were harvested for whole-cell extracts, and aliquots of protein were subjected to SDS-PAGE and immunoblotted with either anti-Setd8 (sc-54996) or anti-H4K20me1 antibody. Equal loading of the proteins was confirmed by the detection of β -actin (ACTB; A5441). (D) 3T3-L1 cells were induced for differentiation for 8 days in the absence (DMSO) or presence of either 20 μ M of T0070907 or 5 μ M of troglitazone (PPAR γ agonist) and analyzed for H4K20me1 modifications by ChIP-qPCR using the specific primers as shown in panel A. (B to D) The data are the averages of three replicates, and the error bars represent the standard errors of the means. (E) PPAR γ 2-expressing NIH 3T3 cells were reinfected with retroviruses carrying the gene for Setd8 and were selected with puromycin. Two-day-postconfluent cells were induced with MDI or troglitazone for 2 days. ORO staining was performed on day 8 of differentiation.

the *Ppar γ 2* promoter and activate histone modifications of the *Ppar γ 2* gene, thereby activating transcription. Our results add a central piece to the puzzle of understanding the transcriptional cascade in adipogenesis and support a model in which a PPAR γ -mediated transcriptional feedback loop through chromatin modification is essential for the transcriptional activation of PPAR γ 2 and the subsequent maturation of adipocytes.

In conclusion, we report that two well-characterized HKMTs, Setdb1 and Setd8, are coordinately regulated by

PPAR γ and that their increased activity facilitates terminal adipocyte differentiation through chromatin modification. We also report that PPAR γ drives the feedback loop induction of the PPAR γ 2 gene and many of the other target genes via two pathways, one through transcription and the other through an epigenetic pathway (as illustrated in Fig. 6). PPAR γ requires Setd8 to acquire H4K20me1 modification in order to enhance its transcription, while Setd8 requires PPAR γ to be transcriptionally induced. These two are both required for the expression of PPAR γ targets. This finding

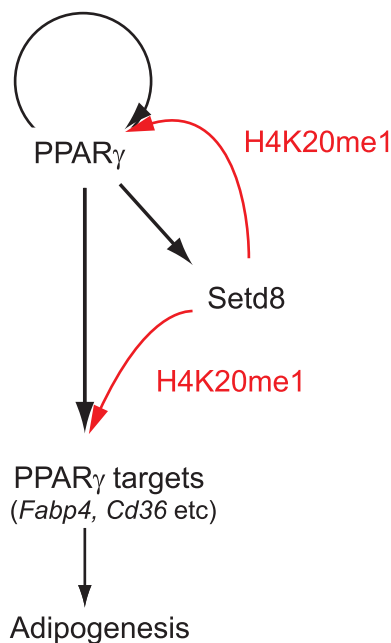


FIG. 6. Models for the coordinate regulation of transcriptions and histone modification by PPAR γ for adipocyte differentiation. PPAR γ transcriptionally activates the Setd8 gene, which in turn increases the H4K20me1 levels of PPAR γ and its targets. PPAR γ also targets PPAR γ 2. These pathways lead to the induction of adipogenic gene expressions and subsequent adipocyte differentiation. The black arrows denote transcriptional pathways, and the red arrows denote pathways of histone modification.

offers new insight into the potential role of PPAR γ in epigenetics and signaling during adipocyte differentiation.

ACKNOWLEDGMENTS

We thank Rob Rawson for critical reading of the manuscript; Takeshi Inagaki for helpful discussion; and Hiroko Meguro, Aoi Uchida, and Hiromi Kudo for technical assistance.

This study was supported in part by the Translational Systems Biology and Medicine Initiative (TSBMI); a Grant-in-Aid for Scientific Research, a grant of the Genome Network Project from the Ministry of Education, Culture, Sports, Science and Technology, Japan; grants from the Program of Fundamental Studies in Health Sciences of the National Institute of Biomedical Innovation (NIBIO); and the NFAT project of New Energy and Industrial Technology Development Organization (NEDO). K.W. is a recipient of the JSPS Research Fellowship for Young Scientists.

REFERENCES

- Barski, A., S. Cuddapah, K. Cui, T. Y. Roh, D. E. Schones, Z. Wang, G. Wei, I. Chepelev, and K. Zhao. 2007. High-resolution profiling of histone methylations in the human genome. *Cell* **129**:823–837.
- Birsoy, K., Z. Chen, and J. Friedman. 2008. Transcriptional regulation of adipogenesis by KLF4. *Cell Metab.* **7**:339–347.
- Reference deleted.
- El-Jack, A. K., J. K. Hamm, P. F. Pilch, and S. R. Farmer. 1999. Reconstitution of insulin-sensitive glucose transport in fibroblasts requires expression of both PPAR γ and C/EBP α . *J. Biol. Chem.* **274**:7946–7951.
- Fajas, L., D. Auboef, E. Raspe, K. Schoonjans, A. M. Lefebvre, R. Saladin, J. Najib, M. Laville, J. C. Fruchart, S. Deeb, A. Vidal-Puig, J. Flier, M. R. Briggs, B. Staels, H. Vidal, and J. Auwerx. 1997. The organization, promoter analysis, and expression of the human PPAR γ gene. *J. Biol. Chem.* **272**:18779–18789.
- Farmer, S. R. 2006. Transcriptional control of adipocyte formation. *Cell Metab.* **4**:263–273.
- Green, H., and O. Kehinde. 1975. An established preadipose cell line and its differentiation in culture. II. Factors affecting the adipose conversion. *Cell* **5**:19–27.
- Hayashi, H., G. Nagae, S. Tsutsumi, K. Kaneshiro, T. Kozaki, A. Kaneda, H. Sugisaki, and H. Aburatani. 2007. High-resolution mapping of DNA methylation in human genome using oligonucleotide tiling array. *Hum. Genet.* **120**:701–711.
- Jaenisch, R., and A. Bird. 2003. Epigenetic regulation of gene expression: how the genome integrates intrinsic and environmental signals. *Nat. Genet.* **33**(Suppl.):245–254.
- Juge-Aubry, C., A. Pernin, T. Favez, A. G. Burger, W. Wahli, C. A. Meier, and B. Desvergne. 1997. DNA binding properties of peroxisome proliferator-activated receptor subtypes on various natural peroxisome proliferator response elements. Importance of the 5'-flanking region. *J. Biol. Chem.* **272**:25252–25259.
- Kaneshiro, K., S. Tsutsumi, S. Tsuji, K. Shirahige, and H. Aburatani. 2007. An integrated map of p53-binding sites and histone modification in the human ENCODE regions. *Genomics* **89**:178–188.
- Katou, Y., K. Kaneshiro, H. Aburatani, and K. Shirahige. 2006. Genomic approach for the understanding of dynamic aspect of chromosome behavior. *Methods Enzymol.* **409**:389–410.
- Kliewer, S. A., B. M. Forman, B. Blumberg, E. S. Ong, U. Borgmeyer, D. J. Mangelsdorf, K. Umeson, and R. M. Evans. 1994. Differential expression and activation of a family of murine peroxisome proliferator-activated receptors. *Proc. Natl. Acad. Sci. USA* **91**:7355–7359.
- Lefterova, M. I., Y. Zhang, D. J. Steger, M. Schupp, J. Schug, A. Cristancho, D. Feng, D. Zhuo, C. J. Stoeckert, Jr., X. S. Liu, and M. A. Lazar. 2008. PPAR γ and C/EBP factors orchestrate adipocyte biology via adjacent binding on a genome-wide scale. *Genes Dev.* **22**:2941–2952.
- Lin, F. T., and M. D. Lane. 1994. CCAAT/enhancer binding protein alpha is sufficient to initiate the 3T3-L1 adipocyte differentiation program. *Proc. Natl. Acad. Sci. USA* **91**:8757–8761.
- Reference deleted.
- Margueron, R., P. Trojer, and D. Reinberg. 2005. The key to development: interpreting the histone code? *Curr. Opin. Genet. Dev.* **15**:163–176.
- Reference deleted.
- Mootha, V. K., C. M. Lindgren, K. F. Eriksson, A. Subramanian, S. Sihag, J. Lehar, P. Puigserver, E. Carlsson, M. Ridderstrale, E. Laurila, N. Houstis, M. J. Daly, N. Patterson, J. P. Mesirov, T. R. Golub, P. Tamayo, B. Spiegelman, E. S. Lander, J. N. Hirschhorn, D. Altshuler, and L. C. Groop. 2003. PGC-1 α -responsive genes involved in oxidative phosphorylation are coordinately downregulated in human diabetes. *Nat. Genet.* **34**:267–273.
- Mori, T., H. Sakaue, H. Iguchi, H. Gomi, Y. Okada, Y. Takashima, K. Nakamura, T. Nakamura, T. Yamauchi, N. Kubota, T. Kadowaki, Y. Matsuki, W. Ogawa, R. Hiramatsu, and M. Kasuga. 2005. Role of Kruppel-like factor 15 (KLF15) in transcriptional regulation of adipogenesis. *J. Biol. Chem.* **280**:12867–12875.
- Mueller, E., S. Drori, A. Ayer, J. Yie, P. Sarraf, H. Chen, S. Hauser, E. D. Rosen, K. Ge, R. G. Roeder, and B. M. Spiegelman. 2002. Genetic analysis of adipogenesis through peroxisome proliferator-activated receptor gamma isoforms. *J. Biol. Chem.* **277**:41925–41930.
- Nielsen, R., T. A. Pedersen, D. Hagenbeek, P. Moulos, R. Siersbaek, E. Megens, S. Denissov, M. Borgesen, K. J. Francoijs, S. Mandrup, and H. G. Stunnenberg. 2008. Genome-wide profiling of PPAR γ :RXR and RNA polymerase II occupancy reveals temporal activation of distinct metabolic pathways and changes in RXR dimer composition during adipogenesis. *Genes Dev.* **22**:2953–2967.
- Ohguchi, H., T. Tanaka, A. Uchida, K. Magoori, H. Kudo, I. Kim, K. Daigo, I. Sakakibara, M. Okamura, H. Harigae, T. Sasaki, T. F. Osborne, F. J. Gonzalez, T. Hamakubo, T. Kodama, and J. Sakai. 2008. Hepatocyte nuclear factor 4 α contributes to thyroid hormone homeostasis by cooperatively regulating the type 1 iodothyronine deiodinase gene with GATA4 and Kruppel-like transcription factor 9. *Mol. Cell. Biol.* **28**:3917–3931.
- Oishi, Y., I. Manabe, K. Tobe, K. Tsushima, T. Shindo, K. Fujiu, G. Nishimura, K. Maemura, T. Yamauchi, N. Kubota, R. Suzuki, T. Kitamura, S. Akira, T. Kadowaki, and R. Nagai. 2005. Kruppel-like transcription factor KLF5 is a key regulator of adipocyte differentiation. *Cell Metab.* **1**:27–39.
- Palomero, T., W. K. Lim, D. T. Odom, M. L. Sulis, P. J. Real, A. Margolin, K. C. Barnes, J. O'Neil, D. Neuberg, A. P. Weng, J. C. Aster, F. Sigaux, J. Soulier, A. T. Look, R. A. Young, A. Califano, and A. A. Ferrando. 2006. NOTCH1 directly regulates c-MYC and activates a feed-forward-loop transcriptional network promoting leukemic cell growth. *Proc. Natl. Acad. Sci. USA* **103**:18261–18266.
- Sakai, J., R. B. Rawson, P. J. Espenshade, D. Cheng, A. C. Seegmiller, J. L. Goldstein, and M. S. Brown. 1998. Molecular identification of the sterol-regulated luminal protease that cleaves SREBPs and controls lipid composition of animal cells. *Mol. Cell* **2**:505–514.
- Subramanian, A., P. Tamayo, V. K. Mootha, S. Mukherjee, B. L. Ebert, M. A. Gillette, A. Paulovich, S. L. Pomeroy, T. R. Golub, E. S. Lander, and J. P. Mesirov. 2005. Gene set enrichment analysis: a knowledge-based approach for interpreting genome-wide expression profiles. *Proc. Natl. Acad. Sci. USA* **102**:15545–15550.
- Takada, I., M. Mihara, M. Suzawa, F. Ohtake, S. Kobayashi, M. Igarashi, M. Y. Youn, K. Takeyama, T. Nakamura, Y. Mezaki, S. Takezawa, Y. Yogiashi, H. Kitagawa, G. Yamada, S. Takada, Y. Minami, H. Shibuya, K.

- Matsumoto, and S. Kato.** 2007. A histone lysine methyltransferase activated by non-canonical Wnt signalling suppresses PPAR-gamma transactivation. *Nat. Cell Biol.* **9**:1273–1285.
29. **Talasz, H., H. H. Lindner, B. Sarg, and W. Helliger.** 2005. Histone H4-lysine 20 monomethylation is increased in promoter and coding regions of active genes and correlates with hyperacetylation. *J. Biol. Chem.* **280**:38814–38822.
30. **Tong, Q., G. Dalgin, H. Xu, C. N. Ting, J. M. Leiden, and G. S. Hotamisligil.** 2000. Function of GATA transcription factors in preadipocyte-adipocyte transition. *Science* **290**:134–138.
31. **Tong, Q., J. Tsai, G. Tan, G. Dalgin, and G. S. Hotamisligil.** 2005. Interaction between GATA and the C/EBP family of transcription factors is critical in GATA-mediated suppression of adipocyte differentiation. *Mol. Cell. Biol.* **25**:706–715.
32. **Tontonoz, P., E. Hu, and B. M. Spiegelman.** 1994. Stimulation of adipogenesis in fibroblasts by PPAR gamma 2, a lipid-activated transcription factor. *Cell* **79**:1147–1156.
33. **Vakoc, C. R., M. M. Sachdeva, H. Wang, and G. A. Blobel.** 2006. Profile of histone lysine methylation across transcribed mammalian chromatin. *Mol. Cell. Biol.* **26**:9185–9195.
34. **Wendt, K. S., K. Yoshida, T. Itoh, M. Bando, B. Koch, E. Schirghuber, S. Tsutsumi, G. Nagae, K. Ishihara, T. Mishiro, K. Yahata, F. Imamoto, H. Aburatani, M. Nakao, N. Imamoto, K. Maeshima, K. Shirahige, and J. M. Peters.** 2008. Cohesin mediates transcriptional insulation by CCCTC-binding factor. *Nature* **451**:796–801.
35. **Xu, Z., S. Yu, C.-H. Hsu, J. Eguchi, and E. D. Rosen.** 2008. The orphan nuclear receptor chicken ovalbumin upstream promoter-transcription factor II is a critical regulator of adipogenesis. *Proc. Natl. Acad. Sci. USA.* doi: 10.1073/pnas.0707082105.
36. **Zhu, Y., C. Qi, J. R. Korenberg, X. N. Chen, D. Noya, M. S. Rao, and J. K. Reddy.** 1995. Structural organization of mouse peroxisome proliferator-activated receptor gamma (mPPAR gamma) gene: alternative promoter use and different splicing yield two mPPAR gamma isoforms. *Proc. Natl. Acad. Sci. USA* **92**:7921–7925.
37. **Zuo, Y., L. Qiang, and S. R. Farmer.** 2006. Activation of CCAAT/enhancer-binding protein (C/EBP) alpha expression by C/EBP beta during adipogenesis requires a peroxisome proliferator-activated receptor-gamma-associated repression of HDAC1 at the C/ebp alpha gene promoter. *J. Biol. Chem.* **281**:7960–7967.